Shock and Vibration 19 (2012) 693–705
DOI 10.3233/SAV-2011-0660
IOS Press

Prediction of turbulent boundary layer induced noise in the cabin of a BWB aircraft

Joana Rocha[a,*], Afzal Suleman[a] and Fernando Lau[b]
[a]*Department of Mechanical Engineering, University of Victoria, Victoria, BC, Canada*
[b]*Departamento de Engenharia Mecânica (Aeroespacial), Instituto Superior Técnico, Lisboa, Portugal*

Received 3 April 2011
Revised 30 October 2011

Abstract. This paper discusses the development of analytical models for the prediction of aircraft cabin noise induced by the external turbulent boundary layer (TBL). While, in previous works, the contribution of an individual panel to the cabin interior noise was considered, here, the simultaneous contribution of multiple flow-excited panels is analyzed. Analytical predictions are presented for the interior sound pressure level (SPL) at different locations inside the cabin of a Blended Wing Body (BWB) aircraft, for the frequency range 0–1000 Hz. The results show that the number of vibrating panels significantly affects the interior noise levels. It is shown that the average SPL, over the cabin volume, increases with the number of vibrating panels. Additionally, the model is able to predict local SPL values, at specific locations in the cabin, which are also affected with by number of vibrating panels, and are different from the average values.

Keywords: Turbulent boundary layer, aircraft cabin noise prediction, fuselage panels

1. Introduction

The structural response to turbulent flow excitation and the radiation of sound by vibrating structures have been a topic of investigation by many authors. These problems are of considerable interest, especially in aircraft, where the structural parts are subjected to fatigue, and the structural vibration being a significant cause of interior cabin noise levels. Even though these topics have been investigated for many years, there is still space for new developments in understanding the mechanisms of sound transmission and radiation involved in these problems. In particular, the TBL has been identified as the major source of interior noise in jet powered aircraft, while in cruise flight [1,2] – refer to Fig. 1 of [1]. Understanding the turbulent boundary layer phenomenon, the induced wall pressure fluctuations, consequent vibration and radiated noise is an ongoing subject of investigation.

Several theoretical, numerical and experimental studies were performed to explore the vibration and radiation of sound from isolated panels (i.e., not coupled with an acoustic cabin), excited by the turbulent flows [3–9]. These investigations provide knowledge about the shape of the power spectrum and space-time correlation of the TBL pressure fluctuations on aircraft panels, as well as displacement and acceleration spectra of the vibrating panels.

Additionally, a number of studies were conducted to investigate structural-acoustic coupled systems excited by random noise or by turbulent flow, consisted by a single panel coupled with a small acoustic enclosure [10–13]. These studies provide a good basis, and were utilized as validation examples in [14], to confirm the analytical predictions obtained for the structural vibration levels and interior noise levels. Several experimental studies were performed by NASA taking into consideration the aircraft interior noise induced by the TBL [15–17]. These studies make experimental data available for the interior SPL and fuselage skin vibrations spectra, at various locations in

*Corresponding author. E-mail: jdarocha@uvic.ca.

ISSN 1070-9622/12/$27.50

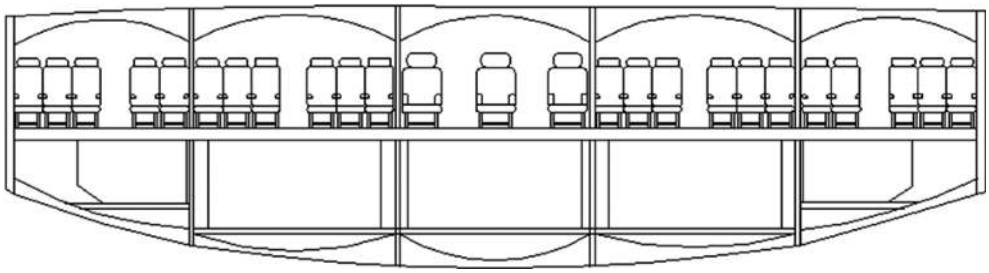

Fig. 1. Cabin section layout of a 5 bay BWB aircraft.

the cabin and cockpit of commercial aircraft, for aluminum and composite fuselages. These measurements are a good validation database for future and more advanced models, capable of predicting interior noise levels for such complex systems.

The TBL has been shown to be a major source of interior noise in jet powered aircraft. Specifically, in [15], interior SPL measurements show that increasing the aircraft speed has a dramatic effect on the TBL-induced noise, as the interior sound levels increase with the flight speed. Additionally, as concluded in [18,19], the TBL wall pressure levels increase with the flight Mach number, and in the absence of hydrodynamic coincidence, the interior SPL usually follows the same tendency [12,20,21]. In the presence of hydrodynamic coincidence, the increased interior SPL with the flight speed is generally valid for frequencies below and above the neighbourhood of the frequency at which hydrodynamic coincidence occurs, as verified in [6].

Nowadays, the TBL wall pressure fluctuations power spectral density is commonly defined using empirical models. The Corcos formulation [22,23] has been widely used for this purpose. Although a number of other models were developed after Corcos model, the Corcos formulation is widely used in recent studies to describe the TBL pressure field, as in [24–27]. Corcos model captures the fundamental pressure tendency along the frequency, requires significantly reduced computational effort to employ, and provides a good estimation for the TBL wall-pressure fluctuations levels at and near the convective peak – which is of fundamental importance for aircraft boundary layers [24]. The main disadvantage of Corcos model is the fact that it does not account with the variation of the boundary layer thickness in the flow direction. In order to overcome this drawback, in the present study the Efimtsov model [28] is used to provide the TBL reference pressure power spectral density (PSD), which considers the boundary layer thickness as a variable. Comparing the several models available to describe the TBL wall pressure PSD [29], the Efimtsov model is a suitable candidate, which provides a good agreement with the experimental data [30].

Motivated by the previous studies, and by the significance of understanding the physics involved in the flow-induced noise problem in real transport vehicle cabins, with rectangular cross section, a three-dimensional analytical model is developed to investigate the coupling between the vibration of a multi-panel wall and a box acoustic cabin. A good example of a rectangular-shaped aircraft cabin section is a 5 bay cabin BWB (Blended-Wing-Body) aircraft, which configuration is shown in Fig. 1 [31]. It is anticipated that the BWB cabin, which has engines mounted at the rear of the fuselage, will not be significantly affected by the jet noise. Instead, the TBL and the engine noise propagation through the fuselage structure should represent the major sources of cabin noise.

In the present study, a BWB cabin bay, filled with air and pressurized, is analyzed. The cabin bay is considered to have five rigid walls and one flexible wall, composed with 50 structural panels. The dimensions and properties of the panels and cabin are similar to those of a typical aircraft structural panel and passenger cabin section, respectively. The TBL excitation is representative of typical cruise conditions of a commercial aircraft, in high subsonic cruise and stabilized flight conditions, and the flow is assumed to be attached and completely developed over the aircraft structure. The amplitude of the wall pressure fluctuations is dependent on the turbulent boundary layer thickness, thus depends on the longitudinal position of the plate.

Previous works were performed by the authors that led to the present investigation. In [14], the base analytical model was validated, considering a single panel coupled with an acoustic enclosure. The analytical framework was successfully validated through the comparison with several independent experimental and numerical studies. Additionally, considering a system with a multi-panel wall vibrating and coupled with a large acoustic cabin, studies were conducted in order to investigate the individual contribution of each plate, located at different positions, to

Table 1
External flow properties (air)

Description	Variable	Value
Speed of sound	c	309.6 m s^{-1}
Air density	ρ	0.54 Kg m^{-3}
Air kinematic viscosity	ν	2.85 $\times$ 10^{-5} m^2 s^{-1}
Free stream velocity	U_∞	229.104 m s^{-1}
TBL convective velocity	U_c	0.7 U_∞
Empirical parameter (x-direction)	α_x	0.1
Empirical parameter (y-direction)	α_y	0.77

the interior SPL. It was shown that plates located at different positions have dissimilar contributions to the cabin interior SPL. In contrast with previous works, the present study investigates the structural-acoustic systems in which several plates are vibrating simultaneously. Several cases, varying the number of vibrating panels, are examined and compared.

2. Mathematical approach

2.1. Turbulent boundary layer empirical model equations

The TBL wall pressure field is usually statistically described in terms of the pressure power spectral density. More specifically, the previously referred models [22–27], were obtained for fully developed turbulent flow over a flat plate, for zero mean pressure gradient. For these conditions, the turbulent flow can be regarded as stationary in time and homogeneous in space. In this case, the cross-spectral density of the wall pressure over the (x, y) plane, for flow in the x-direction, is defined through the Corcos formulation [20,21], as

$$S(x,\xi_x,\xi_y,\omega) = S_{ref}(x,\omega)e^{-\frac{\alpha_x\omega|\xi_x|}{U_c}}e^{-\frac{\alpha_y\omega|\xi_y|}{U_c}}e^{-\frac{i\omega\xi_x}{U_c}}, \tag{1}$$

where $S_{ref}(x,\omega)$ is defined through the Efimtsov model [28] as follows

$$S_{ref}(x,\omega) = \frac{\tau_w^2(x)\delta(x)}{U_\tau(x)}\frac{0.01\pi}{1+0.02\,Sh^{2/3}(x,\omega)}, \tag{2}$$

with:

$$U_\tau(x) = U_\infty\sqrt{\frac{C_f(x)}{2}}, \tau_w(x) = \frac{1}{2}\rho U_\infty^2 C_f(x), \text{ and } Sh(x,\omega) = \frac{\omega\delta(x)}{U_\tau(x)}. \tag{3}$$

In the above equations, ξ_x and ξ_y are the spatial separations from the reference point in the x- and y-directions, ω is the angular frequency, α_x and α_y are the empirical parameters which denote the loss of coherence in the x- and y- directions (in [29], the recommended values for aircraft boundary layers are $\alpha_x = 0.1$ and $\alpha_y = 0.77$), $U_c \approx 0.7$ U_∞ is the TBL convective velocity, U_∞ is the free-stream velocity, $U_\tau(x)$ is the friction velocity, $\tau_w(x)$ is the mean wall shear stress, $C_f(x)$ is the friction coefficient, and $\delta(x)$ is the TBL thickness. For turbulent boundary layers, $C_f(x)$ and $\delta(x)$ may be defined, respectively from [4,32], by

$$C_f(x) = 0.37(\text{Log}_{10}Re_x)^{-2.584}, \text{ and } \delta(x) = 0.37\times Re_x^{-\frac{1}{5}}\left[1+\left(\frac{Re_x}{6.9\times10^7}\right)^2\right]^{\frac{1}{10}}. \tag{4}$$

The external flow parameters used in the present study are shown in Table 1, corresponding to a normal cruise flight conditions, at 25000 ft altitude.

2.2. Structural-acoustic coupled system equations

2.2.1. The single-panel coupled with an acoustic cabin

The structural panel displacement and acoustic enclosure pressure may be defined, through the panels and enclosure natural modes, respectively as follows

$$w(x,y,t) = \sum_{m_x=1}^{M_x} \sum_{m_y=1}^{M_y} \alpha_{m_x}(x)\beta_{m_y}(y)q_{m_x m_y}(t), \tag{5a}$$

and

$$p(x,y,z,t) = \sum_{n_x=1}^{N_x} \sum_{n_y=1}^{N_y} \sum_{n_z=1}^{N_z} \psi_{n_x}(x)\phi_{n_y}(y)\Gamma_{n_z}(z)r_{n_x n_y n_z}(t), \tag{5b}$$

where $\alpha_{m_x}(x)$ and $\beta_{m_y}(y)$ are the $w(x,y,t)$ spatial functions, $q_{m_x m_y}(t)$ are the $w(x,y,t)$ time functions, $\psi_{n_x}(x)$, $\phi_{n_y}(y)$ and $\Gamma_{n_z}(z)$ are the $p(x,y,z,t)$ spatial functions, $r_{n_x n_y n_z}(t)$ are the $p(x,y,z,t)$ spatial time functions, M $=$ M$_x\times$ M$_y$ is the total number of plate modes (m_x, m_y), and N $=$ N$_x\times$N$_y\times$N$_z$ is the total number of acoustics modes (n_x, n_y, n_z). For the simply supported panel and rigid body enclosure, the spatial functions can be defined, respectively, as

$$\alpha_{m_x}(x) = \sqrt{\frac{2}{\mathrm{a}}}\sin\left(\frac{m_x\pi x}{\mathrm{a}}\right), \text{ and } \beta_{m_y}(y) = \sqrt{\frac{2}{b}}\sin\left(\frac{m_y\pi y}{b}\right), \tag{6a}$$

$$\psi_{n_x}(x) = \frac{A_{n_x}}{\sqrt{L_x}}\cos\left(\frac{n_x\pi x}{L_x}\right), \phi_{n_y}(y) = \frac{A_{n_y}}{\sqrt{L_y}}\cos\left(\frac{n_y\pi y}{L_y}\right), \text{ and } \Gamma_{n_z}(z) = \frac{A_{n_z}}{\sqrt{L_z}}\cos\left(\frac{n_z\pi z}{L_z}\right), \tag{6b}$$

in which a is the panel length, b is the panel width, L_x, L_y and L_z are acoustic enclosure length, width and height, respectively, and A_n is $\sqrt{2}$ when $n \neq 0$ and equal to 1 when $n = 0$. As described in more detail in [14], the governing equations on the coupled structural-acoustic system, consisting of a single panel-single acoustic enclosure, results in the following system of equations written in the matrix form:

$$\begin{bmatrix} \mathbf{M}_{pp} & \mathbf{0} \\ \mathbf{M}_{cp} & \mathbf{M}_{cc} \end{bmatrix} \begin{Bmatrix} \ddot{\mathbf{q}}(t) \\ \ddot{\mathbf{r}}(t) \end{Bmatrix} + \begin{bmatrix} \mathbf{D}_{pp} & \mathbf{0} \\ \mathbf{0} & \mathbf{D}_{cc} \end{bmatrix} \begin{Bmatrix} \dot{\mathbf{q}}(t) \\ \dot{\mathbf{r}}(t) \end{Bmatrix} + \begin{bmatrix} \mathbf{K}_{pp} & \mathbf{K}_{pc} \\ \mathbf{0} & \mathbf{K}_{cc} \end{bmatrix} \begin{Bmatrix} \mathbf{q}(t) \\ \mathbf{r}(t) \end{Bmatrix} = \begin{Bmatrix} \mathbf{p}_{tbl}(t) \\ \mathbf{0} \end{Bmatrix} \tag{7}$$

where subscripts p an c stand for $plate$ and $cavity$, $\mathbf{q}(t)$ and $\mathbf{r}(t)$ are the vectors of the considered time functions $q_{m_x m_y}(t)$ and $r_{n_x n_y n_z}(t)$, respectively, $\mathbf{p}_{tbl}(t)$ express the TBL excitation, and $\mathbf{M}$, $\mathbf{D}$, and $\mathbf{K}$ are the mass, damping and stiffness matrices, defined as follows

$$\begin{aligned} &\mathbf{M}_{pp} = \mathrm{diag}[\rho_p h_p], \mathbf{M}_{cc} = \mathrm{diag}\left[\frac{1}{c_0^2}\right], \\ &\mathbf{M}_{cp} = \rho_0\left[\frac{(-1)^{n_z}A_{n_z}}{\sqrt{L_z}}\int_{x_{p_i}}^{x_{p_f}} \alpha_{m_x}(x)\psi_{n_x}(x)\mathrm{dx}\int_{y_{p_i}}^{y_{p_f}} \beta_{m_y}(y)\phi_{n_y}(y)\mathrm{dy}\right], \end{aligned} \tag{8a}$$

$$\mathbf{D}_{pp} = \mathrm{diag}[2\rho_p h_p \omega_m \xi_p], \mathbf{D}_{cc} = \mathrm{diag}\left[2\frac{1}{c_0^2}\omega_n \xi_{ac}\right], \tag{8b}$$

$$\begin{aligned} &\mathbf{K}_{pp} = \mathrm{diag}[\omega_m^2 \rho_p h_p], \mathbf{K}_{cc} = \mathrm{diag}\left[\frac{\omega_n^2}{c_0^2}\right], \\ &\mathbf{K}_{pc} = \left[\frac{-(-1)^{n_z}A_{n_z}}{\sqrt{L_z}}\int_{x_{p_i}}^{x_{p_f}} \alpha_{m_x}(x)\psi_{n_x}(x)dx\int_{y_{p_i}}^{y_{p_f}} \beta_{m_y}(y)\phi_{n_y}(y)dy\right], \end{aligned} \tag{8c}$$

$$\mathbf{p}_{tbl}(t) = -\left[\int_{y_{p_i}}^{y_{p_f}} \int_{x_{p_i}}^{x_{p_f}} \alpha_{m_x}(x)\beta_{m_y}(y)p_{tbl}(x,y,z=L_z,t)\text{dx dy}\right]. \tag{8d}$$

In the above equations, ρ_p and h_p are the density and thickness of the panel, ω_m and ω_n are the natural frequencies of the panel and acoustic enclosure, ξ_p is the plate structural damping ratio, ξ_{ac} is the enclosure acoustic damping ratio, x_{p_i} and x_{p_f} are the initial and last x-coordinates of the plate, y_{p_i} and y_{p_f} are the initial and last y-coordinates of the plate, and c_0 is the speed of sound inside the enclosure. In the frequency domain, ω, Eq. (7) can be written as follows

$$\mathbf{Y}(\omega) = \mathbf{H}(\omega)\mathbf{X}(\omega), \tag{9a}$$

with:

$$\mathbf{Y}(\omega) = \begin{Bmatrix}\mathbf{Q}(\omega)\\ \mathbf{R}(\omega)\end{Bmatrix}, \mathbf{X}(\omega) = \begin{Bmatrix}\mathbf{P}_{tbl}(\omega)\\ \mathbf{0}\end{Bmatrix}, \mathbf{H}(\omega) = \begin{bmatrix}\mathbf{A}\ \mathbf{B}\\ \mathbf{C}\ \mathbf{D}\end{bmatrix}^{-1}, \tag{9b}$$

and

$$\mathbf{A} = -\omega^2\mathbf{M}_{pp} + i\omega\mathbf{D}_{pp} + \mathbf{K}_{pp}, \tag{9c}$$

$$\mathbf{B} = \mathbf{K}_{pc}, \tag{9d}$$

$$\mathbf{C} = -\omega^2\mathbf{M}_{cp}, \tag{9e}$$

$$\mathbf{D} = -\omega^2\mathbf{M}_{cc} + i\omega\mathbf{D}_{cc} + \mathbf{K}_{cc}, \tag{9f}$$

in which $\mathbf{Q}(\omega)$, $\mathbf{R}\ (\omega)$ and $\mathbf{P}_{tbl}\ (\omega)$ are the frequency domain vectors of the $q(t)$, $r(t)$ and $p_{tbl}\ (t)$ vectors defined in the time domain. In the spectral domain, Eq. (9a) can be written as

$$\mathbf{S}_{WW}(\omega) = \mathbf{H}_W{}^*(\omega)\mathbf{S}_{tbl}(\omega)\mathbf{H}_W{}^T(\omega), \tag{10a}$$

and

$$\mathbf{S}_{PP}(\omega) = \mathbf{H}_P{}^*(\omega)\mathbf{S}_{tbl}(\omega)\mathbf{H}_P{}^T(\omega), \tag{10b}$$

where $\mathbf{S}_{WW}\ (\omega)$ is the PSD matrix of the plate displacement, $\mathbf{S}_{PP}\ (\omega)$ is the PSD matrix of the acoustic pressure, $\mathbf{S}_{tbl}\ (\omega)$ is the PSD matrix of the TBL pressure, and superscripts * and T denote Hermitian conjugate and matrix transpose, respectively. Finally, the system response matrices $\mathbf{H}_W\ (\omega)$ and $\mathbf{H}_P\ (\omega)$, and generalized PSD matrix, $\mathbf{S}_{tbl}\ (\omega)$, are defined as follows

$$\mathbf{H}_W(\omega) = (\mathbf{A} - \mathbf{B}\mathbf{D}^{-1}\mathbf{C})^{-1}, \tag{11a}$$

$$\mathbf{H}_P(\omega) = -\mathbf{D}^{-1}\mathbf{C}\mathbf{H}_W(\omega), \tag{11b}$$

$$\mathbf{S}_{tbl}(\omega) = \left[\iint_{y_{p_i}}^{y_{p_f}} \iint_{x_{p_i}}^{x_{p_f}} \alpha_{m_x}(x)\alpha_{m_{x'}}(x')\beta_{m_y}(y)\beta_{m_{y'}}(y')S(x,\xi_x,\xi_y,\omega)\text{dxdx}'\text{dydy}'\right], \tag{11c}$$

in which the term $\mathbf{S}(x,\xi_x,\xi_y,\omega)$ is known from Eq. (1). It is through the $\mathbf{S}_{PP}\ (\omega)$ matrix that is possible to determine the PSD of the acoustic enclosure pressure, in a specific point inside the enclosure as

$$\mathbf{S}_{pp}(x_1, y_1, z_1, x_2, y_2, z_2, \omega) = \sum_{n_{x_1}, n_{x_2}=1}^{N_x^2} \sum_{n_{y_1}, n_{y_2}=1}^{N_y^2} \sum_{n_{z_1}, n_{z_2}=1}^{N_z^2} \psi_{n_{x_1}}(x_1)\psi_{n_{x_2}}(x_2)\phi_{n_{y_1}}(y_1)\phi_{n_{y_2}}(y_2)\Gamma_{n_{z_1}}(z_1)\Gamma_{n_{z_2}}(z_2)\mathbf{S}_{PP}(\omega)_{n_1,n_2} \tag{12}$$

or space-averaged in the acoustic enclosure volume as

$$\mathbf{S}_{pp}(\omega) = \iiint_0^{L_z} \iiint_0^{L_y} \iiint_0^{L_x} \mathbf{S}_{pp}(x_1, y_1, z_1, x_2, y_2, z_2, \omega) \mathrm{dx_1 dx_2 dy_1 dy_2 dz_1 dz_2}. \tag{13}$$

2.2.2. The multi-panel wall coupled with an acoustic cabin

Regarding the system consisted by a single acoustic enclosure coupled with several vibrating panels, the basic model presented previously needs to be modified. Shall one consider N_p plates, part of the same enclosure flexible, and all vibrating due to the TBL excitation, it can be shown that the system governing equations, defined in Eq. (7) for one panel, becomes:

$$\underbrace{\begin{bmatrix} \mathbf{M}_{1_{pp}} & 0 & \dots & 0 & 0 & 0 \\ 0 & \mathbf{M}_{2_{pp}} & \dots & 0 & 0 & 0 \\ \vdots & \vdots & \ddots & \vdots & \vdots & \vdots \\ 0 & 0 & \dots & \mathbf{M}_{N_p-1_{pp}} & 0 & 0 \\ 0 & 0 & \dots & 0 & \mathbf{M}_{N_{p_{pp}}} & 0 \\ \mathbf{M}_{1_{cp}} & \mathbf{M}_{2_{cp}} & \dots & \mathbf{M}_{N_p-1_{cp}} & \mathbf{M}_{N_{p_{cp}}} & \mathbf{M}_{cc} \end{bmatrix}}_{\mathbf{M}} \begin{Bmatrix} \ddot{q}_1(t) \\ \ddot{q}_2(t) \\ \vdots \\ \ddot{q}_{N_p-1}(t) \\ \ddot{q}_{N_p}(t) \\ \ddot{r}(t) \end{Bmatrix} + \underbrace{\begin{bmatrix} \mathbf{D}_{1_{pp}} & 0 & \dots & 0 & 0 & 0 \\ 0 & \mathbf{D}_{2_{pp}} & \dots & 0 & 0 & 0 \\ \vdots & \vdots & \ddots & \vdots & \vdots & \vdots \\ 0 & 0 & \dots & \mathbf{D}_{N_p-1_{pp}} & 0 & 0 \\ 0 & 0 & \dots & 0 & \mathbf{D}_{N_{p_{pp}}} & 0 \\ 0 & 0 & \dots & 0 & 0 & \mathbf{D}_{cc} \end{bmatrix}}_{\mathbf{D}} \begin{Bmatrix} \dot{q}_1(t) \\ \dot{q}_2(t) \\ \vdots \\ \dot{q}_{N_p-1}(t) \\ \dot{q}_{N_p}(t) \\ \dot{r}(t) \end{Bmatrix}$$

$$+ \underbrace{\begin{bmatrix} \mathbf{K}_{1_{pp}} & 0 & \dots & 0 & 0 & \mathbf{K}_{1_{pc}} \\ 0 & \mathbf{K}_{2_{pp}} & \dots & 0 & 0 & \mathbf{K}_{2_{pc}} \\ \vdots & \vdots & \ddots & \vdots & \vdots & \vdots \\ 0 & 0 & \dots & \mathbf{K}_{N_p-1_{pp}} & 0 & \mathbf{K}_{N_p-1_{pc}} \\ 0 & 0 & \dots & 0 & \mathbf{K}_{N_{p_{pp}}} & \mathbf{K}_{N_{p_{pc}}} \\ 0 & 0 & \dots & 0 & 0 & \mathbf{K}_{cc} \end{bmatrix}}_{\mathbf{K}} \begin{Bmatrix} q_1(t) \\ q_2(t) \\ \vdots \\ q_{N_p-1}(t) \\ q_{N_p}(t) \\ r(t) \end{Bmatrix} = \begin{Bmatrix} p_{1_{tbl}}(t) \\ p_{2_{tbl}}(t) \\ \vdots \\ p_{N_p-1_{tbl}}(t) \\ p_{N_{p_t bl}}(t) \\ 0 \end{Bmatrix} \tag{14}$$

where $\mathbf{M}_{i_{pp}}$ and $\mathbf{M}_{i_{cp}}$ are mass matrices of the ith plate, $\mathbf{D}_{i_{pp}}$ is the damping matrix of the ith plate, $\mathbf{K}_{i_{pp}}$ and $\mathbf{K}_{i_{pc}}$ are stiffness matrices of the i^{th} plate. Note that, since $\mathbf{M}_{i_{pp}}$, $\mathbf{D}_{i_{pp}}$, and $\mathbf{K}_{i_{pp}} \in \mathcal{R}^{M\times M}$, $\mathbf{M}_{i_{cp}} \in \mathcal{R}^{N\times M}$, $\mathbf{K}_{i_{pc}} \in \mathcal{R}^{M\times N}$, and $\mathbf{M}_{cc}$, $\mathbf{D}_{cc}$ and $\mathbf{K}_{cc} \in \mathcal{R}^{N\times N}$, it results that $\mathbf{M}$, $\mathbf{D}$ and $\mathbf{K} \in \mathcal{R}^{\{(Np\times M)+N\}\times\{(Np\times M)+N\}}$. Now, writing the governing equations in the frequency domain, and similarly to Eq. (9), it becomes:

$$\mathbf{Y}(\omega) = \mathbf{H}(\omega)\mathbf{X}(\omega), \tag{15a}$$

in which:

$$\mathbf{Y}(\omega) = \begin{Bmatrix} \mathbf{Q}_1(\omega) \\ \mathbf{Q}_2(\omega) \\ \vdots \\ \mathbf{Q}_{N_p-1}(\omega) \\ \mathbf{Q}_{N_p}(\omega) \\ \mathbf{R}(\omega) \end{Bmatrix}, \mathbf{X}(\omega) = \begin{Bmatrix} \mathbf{P}_{1_{tbl}}(\omega) \\ \mathbf{P}_{2_{tbl}}(\omega) \\ \vdots \\ \mathbf{P}_{N_p-1_{tbl}}(\omega) \\ \mathbf{P}_{N_{p_{tbl}}}(\omega) \\ 0 \end{Bmatrix}, \mathbf{H}(\omega) = \begin{bmatrix} \mathbf{A} & \mathbf{B} \\ \mathbf{C} & \mathbf{D} \end{bmatrix}^{-1}, \tag{15b}$$

and

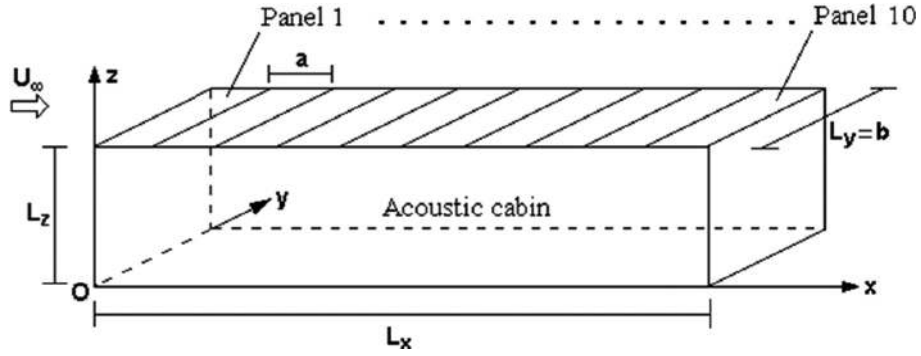

Fig. 2. Configuration of a simple multi-panel wall cabin, composed by 10 panels.

$$\mathbf{A} = \begin{bmatrix} \mathbf{A}_1 & 0 & \dots & 0 & 0 \\ 0 & \mathbf{A}_2 & \dots & 0 & 0 \\ \vdots & \vdots & \ddots & \vdots & \vdots \\ 0 & 0 & \dots & \mathbf{A}_{N_p-1} & 0 \\ 0 & 0 & \dots & 0 & \mathbf{A}_{N_p} \end{bmatrix}, \text{ with } \mathbf{A}_i = -\omega^2 \mathbf{M}_{i_{pp}} + i\omega \mathbf{D}_{i_{pp}} + \mathbf{K}_{i_{pp}}, \tag{15c}$$

$$\mathbf{B} = [\mathbf{B}_1 \ \mathbf{B}_2 \ \dots \ \mathbf{B}_{N_p-1} \ \mathbf{B}_{N_p}]^T, \text{ with } \mathbf{B}_i = \mathbf{K}_{i_{pc}}, \tag{15d}$$

$$\mathbf{C} = [\mathbf{C}_1 \ \mathbf{C}_2 \ \dots \ \mathbf{C}_{N_p-1} \ \mathbf{C}_{N_p}], \text{ with } \mathbf{C}_i = -\omega^2 \mathbf{M}_{i_{cp}}, \tag{15e}$$

$$\mathbf{D} = -\omega^2 \mathbf{M}_{cc} + i\omega \mathbf{D}_{cc} + \mathbf{K}_{cc}, \tag{15f}$$

where $\mathbf{A} \in \mathcal{R}^{(Np\times M)\times(Np\times M)}$, $\mathbf{B} \in \mathcal{R}^{(Np\times M)\times N}$ $\mathbf{C} \in \mathcal{R}^{N\times(Np\times M)}$, and $\mathbf{D} \in \mathcal{R}^{N\times N}$. The matrices $\mathbf{S}_{WW}(\omega)$ and $\mathbf{S}_{PP}(\omega)$ are obtained as in Eqs (10a) and (10b), $\mathbf{H}_W(\omega)$ and $\mathbf{H}_P(\omega)$ through Eqs (11a) and (11b), and the matrix PSD matrix for the multi-panel single-enclosure system, $\mathbf{S}_{tbl}(\omega) \in \mathcal{R}^{(Np\times M)\times(Np\times M)}$, is defined as follows

$$\mathbf{S}_{tbl}(\omega) = \begin{bmatrix} \mathbf{S}_{1_{tbl}}(\omega) & 0 & \dots & 0 & 0 \\ 0 & \mathbf{S}_{2_{tbl}}(\omega) & \dots & \vdots & \vdots \\ \vdots & \vdots & \ddots & \vdots & \vdots \\ 0 & 0 & \dots & \mathbf{S}_{N_p-1\,tbl}(\omega) & 0 \\ 0 & 0 & \dots & 0 & \mathbf{S}_{N_p\,tbl}(\omega) \end{bmatrix}, \tag{16}$$

with each $\mathbf{S}_{i_{tbl}}(\omega) \in \mathcal{R}^{M\times M}$ representing the TBL excitation matrix for the ith plate, and defined by Eq. (11c). After determining these matrices the acoustic enclosure pressure PSD can be calculated from Eqs (12) and (13), respectively for local and average values.

3. Predicted flow-induced noise in BWB aircraft cabin

3.1. Model verification

In the present Section, the analytical model presented in the previous Section is used to predict the interior noise inside a simpler cabin, which configuration is shown in Fig. 2. The predictive results are obtained for four different cases, as following: (a) acoustic cabin coupled only with panel 1; (b) acoustic cabin coupled with panels 1 to 4; (c) acoustic cabin coupled with panels 1 to 6; and (d) acoustic cabin coupled with all 10 panels. The case (a) is the

Table 2
Properties of the physical system in Fig. 2

Description	Variable	Value
External flow speed of sound	c	310 m s^{-1}
External air density	ρ	0.42 Kg m^{-3}
Free stream velocity	U_∞	0.8 c
TBL convective velocity	U_c	0.6 U_∞
Empirical parameter (x-direction)	α_x	0.1
Empirical parameter (y-direction)	α_y	0.5
Plate density	ρ_p	2800 Kg m^{-3}
Plate Elasticity Modulus	E_p	7.0×10^{10} Pa^2
Plate Poisson's ratio	ν_p	0.3
Structural damping ratio	ξ_p	0.01
Plate length	a	0.3 m
Plate width	b	0.3 m
Plate thickness	h_p	0.0018 m
Internal air speed of sound	c_0	310 m s^{-1}
Internal air density	ρ_0	0.42 Kg m^{-3}
Acoustic damping ratio	ξ_{ac}	0.05
Acoustic enclosure length	L_x	3.0 m
Acoustic enclosure width	L_y	0.3 m
Acoustic enclosure height	L_z	0.3 m

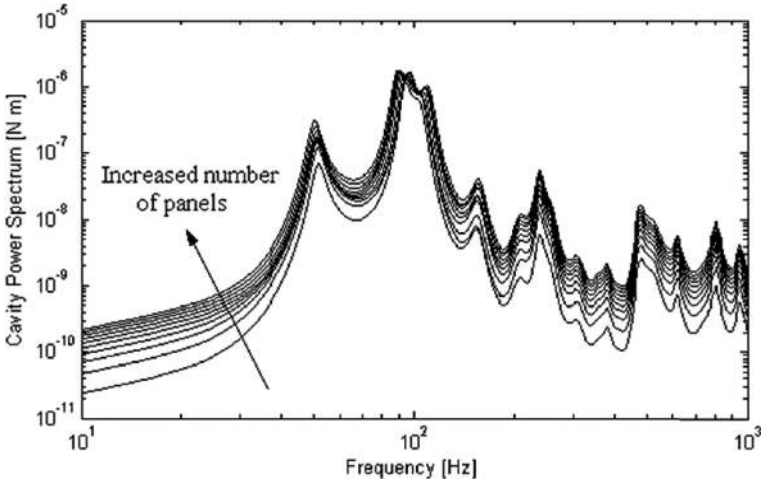

Fig. 3. Cavity power spectrum (average over the cabin volume), by increasing the number of panels from 1 to 10.

base model, from [2], and was used as a validation case in [14]. The properties of the system shown in Fig. 2 are presented in Table 2.

The results for the cavity power spectrum were calculated through the acoustic cabin pressure power spectral density, S_{pp}, as follows

$$E_{pp} = \frac{L_x L_y L_z}{4\rho_0 c_0^2}\omega S_{pp}, \tag{17}$$

for frequencies up to 1000 Hz. For this frequency range, a total number of 20 plate modes ($M_x = 4$ and $M_y = 5$), and 189 acoustic modes ($N_x = 21$, $N_y = 3$ and $N_z = 3$) were necessary to achieve convergence of the spectral quantities. The results for the average E_{pp} (averaged over the enclosure volume) are shown in Fig. 3, increasing the number of vibrating panels from 1 to 10. As expected, the average cavity power spectrum increases with the number of vibrating plates, and the curve maintains a similar shape since all plates have the same properties and dimensions. As shown in previous works, the peaks on the cavity power spectrum curve correspond to both plate and acoustic natural modes.

Table 3
Properties of the physical system in Fig. 5

Description	Variable	Value
Plate density	ρ_p	2800 Kg m^{-3}
Plate Elasticity Modulus	E_p	7.24×10^{10} Pa^2
Plate Poisson's ratio	ν_p	0.33
Structural damping ratio	ξ_p	0.01
Plate length	a	0.5 m
Plate width	b	0.22 m
Plate thickness	h_p	0.00102 m
Plate longitudinal tension	T_x	29300 N m^{-1}
Plate lateral tension	T_y	62100 N m^{-1}
Internal air speed of sound	c_0	340 m s^{-1}
Internal air density	ρ_0	1.2 Kg m^{-3}
Acoustic damping ratio	ξ_{ac}	0.01
Acoustic enclosure length	L_x	2.5 m
Acoustic enclosure width	L_y	2.2 m
Acoustic enclosure height	L_z	2.1 m

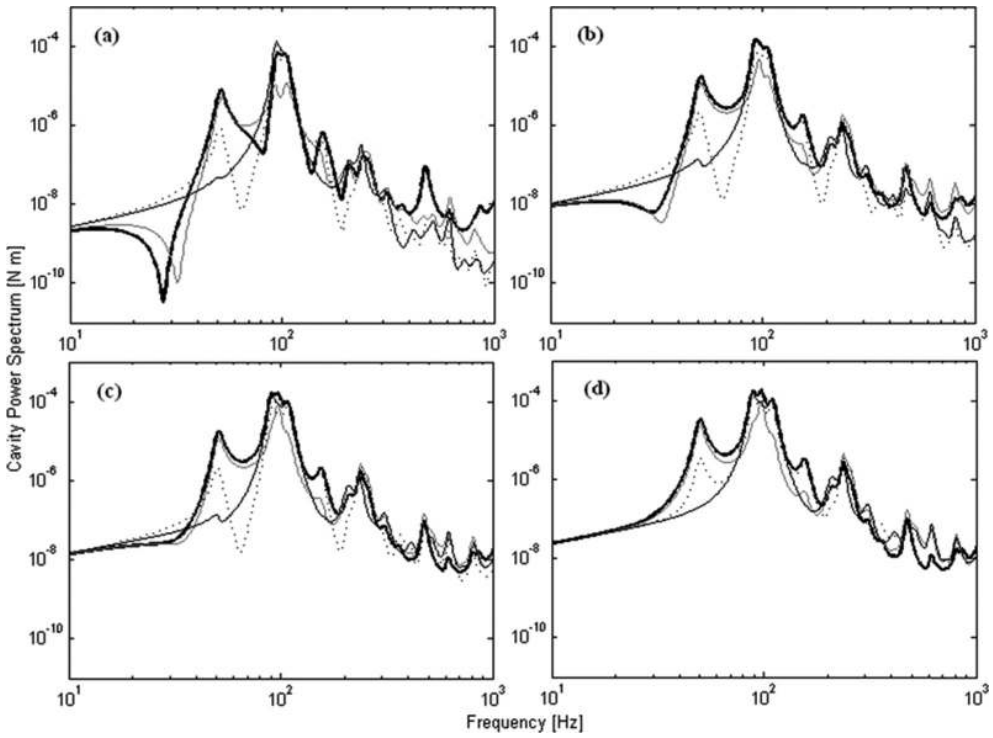

Fig. 4. Cavity power spectrum considering (a) 1 plate, (b) 4 plates, (c) 6 plates, and (d) 10 plates, at 4 points: — (a/2;b/2;L$_z$/2), — (2a;b/2;L$_z$/2), — (L$_x$/2;b/2;L$_z$/2), ... (L$_x$/2+a;b/2;L$_z$/2).

Figure 4 shows the cavity power spectrum prediction at four locations inside the enclosure. As can be seen, as the number of vibrating plates is increased from (a) 1 to (d) 10, the cavity power spectrum also increases in all four locations. Additionally, as the number of vibrating panels increase, the curves peaks and valleys become less evident. Specifically, considering point 1, as the number of plates increase the curve shape becomes gradually more similar with the curve for the average cavity power spectrum, shown in Fig. 3. This way, the model is able to predict local and average values of interior noise, and for a variable number of vibrating panels. As shown in Fig. 4, for a specific point in the enclosure, the number of vibrating panels significantly affects the prediction of interior noise, and this is an important factor in the cabin noise prediction and aircraft design.

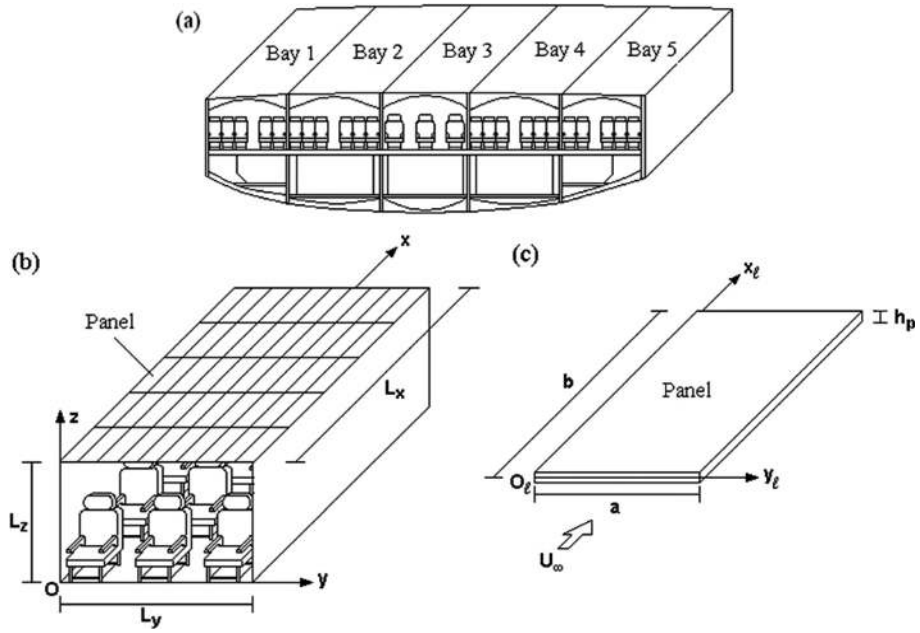

Fig. 5. General BWB aircraft cabin layout: (a) 5 bay cabin cross section, (b) bay 3 schematic: multi-panel wall and box-type cabin, (c) structural panel configuration.

3.2. BWB aircraft cabin results

The cross section shape of a Blended Wing Body aircraft cabin is approximately rectangular, as illustrated in Fig. 5. Figure 5(a) shows the schematic configuration of a 5 bay BWB aircraft fuselage section, with each bay being a single and separate passenger compartment. Figure 5(b) shows the configuration of a single bay, in which the upper wall is considered to be composed by 50 identical structural panels (fuselage skin panels), with 5 panel rows along the x-direction, and 10 panel rows in y-direction. In order to investigate the interior noise induced by the external fully developed TBL, it is assumed that the aircraft fuselage section, shown in Fig. 5(a), is located at a distance of 9.14 m from the aircraft nose. The characteristics of the external flow are shown in Table 1, and the properties of the physical system are given in Table 3, which are similar to those of a real aircraft. The passenger cabin compartment is assumed to be pressurized, and the results were obtained from frequencies up to 1000 Hz. In order to achieve convergence of the calculated spectral quantities up to this frequency, a total number of 44 plate modes ($M_x = 11$ and $M_y = 4$) and 2912 acoustic modes ($N_x = 16$, $N_y = 14$ and $N_z = 13$) is necessary to be considered in the analysis.

Figure 6 shows the variation of the average cabin pressure sound pressure level (averaged over the cabin volume), as a function of the frequency. The results show that, as the number of vibrating panels is increased from 1 to 20, and 20 to 50, an overall increase of the average interior SPL is also observed. As concluded for the simple case analyzed in Section 3.1, the shape of the SPL curve is maintained, as all panels have the same properties. This would not happen if the panels would have different dimensions or properties among them, which can also be obtained through the model presented in Section 2. Some of the peaks in Fig. 6 correspond to the plate's natural frequencies, while others correspond to acoustic natural frequencies, showing the importance of the structural-acoustic coupling for the accurate prediction of cabin interior noise.

To assess the noise levels at specific interior locations in the cabin, the local values of SPL should be calculated. This is particularly important in the estimation of the cabin locations where the passengers will be more negatively affected by the TBL-induced noise. Figure 7 shows the results obtained for four different locations in the BWB aircraft cabin, considering three cases: 1 panel vibrating, i.e., panel (1, 1); 20 panels vibrating, i.e., from panel (1, 1) to panel (2, 10); and 50 panels vibrating, i.e., all panels in the upper wall, from (1, 1) to (5, 10). The cabin interior

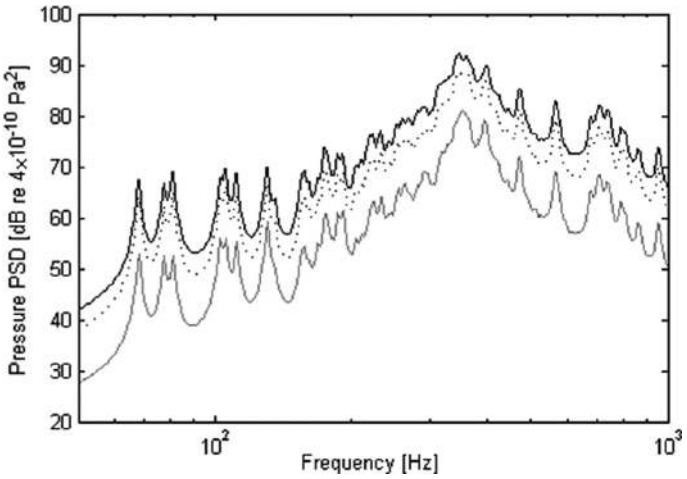

Fig. 6. Average power spectral density of the cabin interior pressure (average over the cabin volume), for: — 1 panel, ... 20 panels, and — 50 panels.

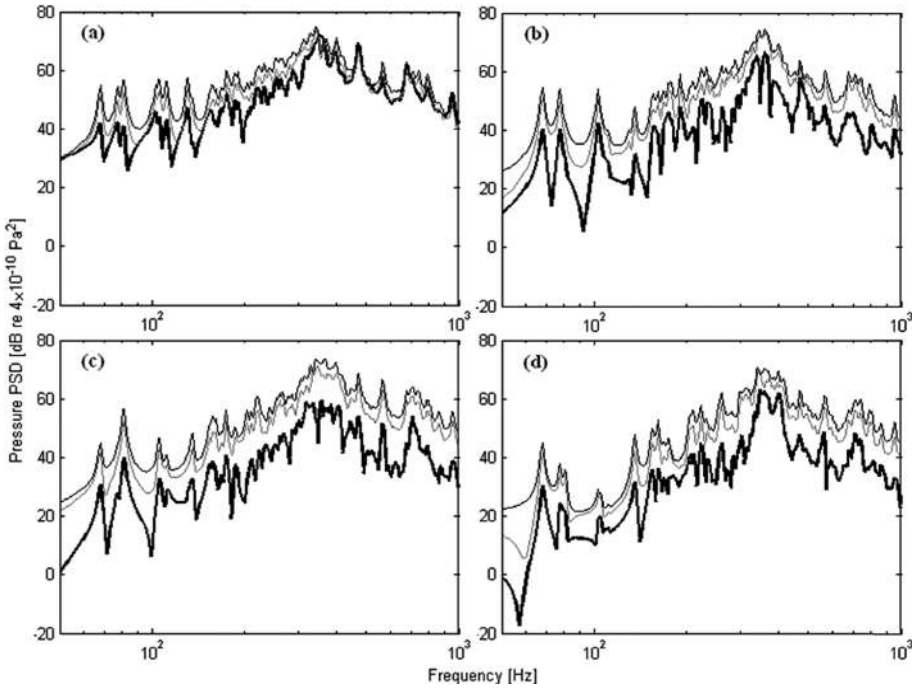

Fig. 7. Power spectral density of the cabin pressure, at (a) point 1: (a/2;b/2;2), (b) point 2: (a/2;b/2;1), (c) point 3: (1;1;2), and (d) point 4: (1;1;1). Comparison among 3 cases: — 1 panel, — 20 panels, and — 50 panels.

points under study are: $(x_1, y_1, z_1) =$ (a/2, b/2, 2), $(x_2, y_2, z_2) =$ (a/2, b/2, 1), $(x_3, y_3, z_3) = (1, 1, 2)$, and $(x_4, y_4, z_4) = (1, 1, 1)$.

Observing the results in Fig. 7, it can be concluded that considering only panel (1,1) vibrating, the results in the four locations differ significantly from one another. However, when considering the 50 panels vibrating, the SPL curves for the four locations are similar for frequencies greater than 355.45 Hz, i.e., for frequencies above the first panel's mode. For frequencies below 355.45 Hz, the same does not occur, with curves having dissimilar shapes in the four points. In the frequency range]0; 355.45] Hz, the peaks in the SPL curve correspond to the acoustic natural modes. Even though the SPL values are smaller in this frequency range, compared with the level for the 355.45 Hz

peak, some of the SPL peaks lying in this range correspond to almost 60 dB SPL in the 50 panel's configuration. This can be of particular interest, since these peaks lie in the human audible range, creating tones and directly affecting the passenger's comfort. It is also important to verify that, depending on the location, these peaks have different amplifications, with their importance shifting from point to point. For instance, point 3 has more amplification on the 2nd peak compared with the 1st peak, the opposite is observed in point 4.

The accuracy of the predicted cabin SPL can be of crucial importance. In particular, the earlier knowledge about which locations in the cabin have more noise amplification, and at which frequencies, can be important for the implementation of noise control techniques. Motivated by this, the present model allows the user to predict the cabin interior noise, induced by the TBL, in the desired locations. Furthermore, the model can easily be used to investigate other systems, by simply changing the properties and dimensions of the panels and acoustic cabin, and also varying the number of vibrating panels. Since changing the number of vibrating panels, and their properties, can significantly affect the interior SPL, the present model can also be used as a basis for a multidisciplinary design optimization analysis, in order to find the best configuration of structural panels and acoustic cabin.

4. Conclusions

In the present work, an analytical model for the prediction of TBL-induced noise in a rectangular aircraft cabin, with multi-panel wall, is presented. Interior noise levels (average and local) were obtained for different locations in the cabin. The effect of the number of vibrating panels in the predicted SPL was analyzed. Results were obtained for a simple cabin, and for a more complex cabin, composed by 50 panels. The characteristics of the external flow, structural panel and acoustic cabin were chosen in order to represent a real aircraft cabin in cruise and stabilized flight.

The predictive results show that the cabin interior noise levels are significantly affected by the number of vibrating panels. For frequencies up to 1000 Hz, the average SPL values show an overall increase with the number of panels. Additionally, as the numbers of panels increase, the SPL curve essentially maintains the same shape, if all the vibrating panels have the same properties. Local SPL values, in specific locations inside the cabin, are also affected by the number of vibrating panels. The local SPL results show that, as the number of vibrating panels is increased, the local SPL curves and values become more similar among the several locations, for frequencies above the first panel resonance. However, for frequencies below this resonance, where the acoustic modes are dominant, the same does not happen. In that range, the SPL curves are different from point to point, which show dissimilar amplifications of the several acoustic modes.

The presented analytical model can be used to study a broad range of different systems involving a rectangular cabin coupled with several vibrating panels, excited by the TBL. The properties of the flow, acoustic cabin, and panels, as well as the number of vibrating panels, can be easily changed to represent other systems. These abilities of the model make it a solid basis for future investigations involving the implementation of noise reduction techniques and multidisciplinary design optimization analyzes. The model can also be modified in order to account for other sources of noise.

Acknowledgements

The authors wish to thank for the financial support of the Foundation for Science and Technology, through a post-graduate scholarship program.

References

[1] D.E. Bishop, Cruise flight noise levels in a turbojet transport airplane, *Noise Control* **7**(2) (1961), 37–42.

[2] K.D. Frampton and R.L. Clark, Power flow in an aeroelastic plate backed by a reverberant cavity, *Journal of the Acoustical Society of America* **102**(3) (1997), 1620–1627.

[3] L. Maestrello, Measurement of noise radiated by turbulent boundary layer excited panels, *Journal of Sound and Vibration* **2**(2) (1965), 100–115.
[4] D.A. Bies, A review of flight and wind tunnel measurements of boundary layer pressure fluctuations and induced structural response, *NASA CR-626*, 1966.
[5] H.G. Davies, Sound from turbulent-boundary-layer-excited panels, *Journal of the Acoustical Society of America* **49**(3) (1971), 878–889.
[6] J.F. Wilby and F.L. Gloyna, Vibration measurements of an airplane fuselage structure I. Turbulent boundary layer excitation, *Journal of Sound and Vibration* **23**(4) (1972), 443–466.
[7] F. Han, R.J. Bernhard and L.G. Mongeau, Prediction of flow-induced structural vibration and sound radiation using energy flow analysis, *Journal of Sound and Vibration* **227**(4) (1999), 685–709.
[8] M. Allen and N. Vlahopoulos, Noise generated from a flexible and elastically supported structure subject to turbulent boundary layer flow excitation, *Finite Elements in Analysis and Design* **37** (2001), 687–712.
[9] B. Liu, Noise radiation of aircraft panels subjected to boundary layer pressure fluctuations, *Journal of Sound and Vibration* **314** (2008), 693–711.
[10] C.K. Barton and E.F. Daniels, Noise transmission through flat rectangular panels into a closed cavity, *NASA TP-1321*, 1978.
[11] C.M. Heatwole, R.J. Bernhard and M.A. Francheck, Robust feedback control of flow induced structural radiation of sound, *NASA Report 0278-1*, 1997.
[12] K.D. Frampton and R.L. Clark, Power flow in an aeroelastic plate backed by a reverberant cavity, *Journal of the Acoustical Society of America* **102**(3) (1997), 1620–1627.
[13] G.C. Smith, R.L. Clark and K.D. Frampton, Optimal tranducer placement for active control of sound transmission through aeroelastic plates, *Journal of the Intelligent Material Systems and Structures* **9** (1998), 975–987.
[14] J. da Rocha, A. Suleman and F. Lau, Prediction of flow-induced noise in transport vehicles: development and validation of a coupled structural-acoustic analytical framework, *Canadian Acoustics* **37**(4) (2009), 13–29.
[15] A.C. Jackson, F.J. Balena, W.L. LaBarge, G. Pei, W.A. Pitman and G. Wittlin, Transport composite fuselage technology – impact dynamics and acoustic transmission, *NASA CR-4035*, 1986.
[16] S.A. Rizzi, R.G. Rackl, J. Cline and E.V. Andrianov, Flight test measurements from the Tu-144LL structure/cabin noise experiment, *NASA TM-209858*, 2000.
[17] T.H. Beier, W.V. Bhat, S.A. Rizzi, R.J. Silcox and M.A. Simpson, High speed research program structural acoustics multi-year summary report, *NASA TM-213536*, 2005.
[18] W.V. Bhat, Flight test measurement of exterior turbulent boundary layer pressure fluctuations on Boeing Model 737 airplane, *Journal of Sound and Vibration* **14**(4) (1971), 439–457.
[19] J.F. Wilby and F.L. Gloyna, Vibration measurements of an airplane fuselage structure II. Jet noise excitation, *Journal of Sound and Vibration* **23**(4) (1972), 467–486.
[20] G.P. Gibbs, R.H. Cabell and J. Juang, Controller Complexity for Active Control of Turbulent Boundary-Layer Noise from Panels, *AIAA Journal* **42**(7) (2004), 1314–1320.
[21] C. Maury, P. Gardonio and S.J. Elliot, A wavenumber approach to modeling the response of a randomly excited panel, part II: application to aircraft panels excited by a turbulent boundary layer, *Journal of Sound and Vibration* **252**(1) (2002), 115–139.
[22] G.M. Corcos, Resolution of pressure in turbulence, *Journal of the Acoustical Society of America* **35**(2) (1963), 192–199.
[23] G.M. Corcos, The structure of the turbulent pressure field in boundary-layer flows, *Journal of Fluid Mechanics* **18** (1964), 353–378.
[24] C. Maury, P. Gardonio and S.J. Elliot, Active control of the flow-induced noise transmitted through a panel, *AIAA Journal* **39**(10) (2001), 1860–1867.
[25] F. Han, L.G. Mongeau and R.J. Bernhard, A model for the vibro-acoustic response of plates excited by complex flows, *Journal of Sound and Vibration* **246**(5) (2001), 901–926.
[26] C. Maury, P. Gardonio and S.J. Elliot, Model for the active control of flow-induced noise transmitted through double partitions, *AIAA Journal* **40**(6) (2002), 1113–1121.
[27] S.J. Elliot, C. Maury and P. Gardonio, The synthesis of spatially correlated random pressure fields, *Journal of the Acoustical Society of America* **117**(3) (2005), 1186–1201.
[28] B.M. Efimtsov, Characteristics of the field of turbulent wall pressure fluctuations at large Reynolds numbers, *Soviet Physics Acoustics* **28**(4) (1982), 289–292.
[29] W.R. Graham, A comparison of models for the wavenumber frequency spectrum of turbulent boundary layer pressures, *Journal of Sound and Vibration* **206**(4) (1997), 541–565.
[30] R. Rackl and A. Weston, Modeling of turbulent boundary layer surface pressure fluctuation auto and cross spectra – verification and adjustments based on TU-144LL data, *NASA CR-213938*, 2005.
[31] V. Mukhopadhyay, Blended-Wing-Body (BWB) fuselage structural design for weight reduction, AIAA-2005-2349, in: *46th AIAA/ASME/ASCE/AHS/ASC Structures, Structural Dynamics and Materials Conference*, Austin, Texas, April 2005, pp. 18–21.
[32] R. Wahidi, W. Chakroun and S. Al-Fahed, The behavior of the skin friction coefficient of a turbulent boundary layer flow over a flat plate with differently configured transverse square grooves, *Experimental Thermal and Fluid Science* **30**(2) (2005), 141–152.